Meeting: 202407 Annual Assembly **Tags:** Scientific document

XY-ZWTQ-2024

A novel monitoring and characterization approach of dynamic wire feeding in GTAW process

Ivan O. Pigozzo[1,a,d], Regis H. G e Silva[1,b,e], Alberto B. Viviani[1,c,f],

[1] LABSOLDA – Welding and Mechatronics Institute (Federal University of Satan Catarina – Brazil)
[a]ivan.pigozzo@posgrad.ufsc.br, [b]regis.silva@ufsc.br, [c]alberto@labsolda.ufsc.br
[d]0000-0002-3866-7885, [e]0000-0003-0660-6495, [f]0000-0002-0303-6792

Abstract

Recent developments in welding technology have focused on the advances of new variants and technique for existing processes, whereby the GTAW with Dynamic Wire Feeding (GTAW-DWF) stands out. The use of automated and more complex processes also demands better methods and more accurate tools for monitoring and controlling. Despite this demand, the relating few works available in the literature handle, mainly, with the influences of the dynamic wire feeding technique over the weld beads. The present work introduces a novel approach to monitor and characterize the GTAW process with dynamic wire feeding. By means of welding data acquisition and high-speed videography and data post-processing, the metal transfer, process stability and wire insertion position were evaluated. The coupled monitoring of the electrode-to-wire voltage and the wire feed speed proved to be an effective tool to accurately define and measure the metal transfer cycles. With the data post-processing algorithms, the metal transfer events in the dynamic wire feeding were characterized by parameters specifically inherent to the technique, such as volume of wire transferred per cycle, bridging time, molten pool elongation, wire dip into the molten pool, maximum and average forward/backward speeds and so on. Furthermore, electrical signals can also be used to monitor the wire insertion position. In this work, it could be established that the electrode-to-wire voltage varies with the electrode-to-wire distance and oscillation amplitude. Moreover, the behavior of electrical and wire feed speed signals also express process instabilities in the metal transfer such as wire stubbing, lack of filler metal and metal transfer irregularity. Abrupt increase or reduction rates of the acquired signals can express distinct phenomena, and the right interpretation can be used to predict or prevent instabilities enhancing the process robustness and reliability.

Keywords

Dynamic wire feeding; GTAW; Metal Transfer; Process Monitoring.

1. Introduction

The automation of Gas Tungsten Arc Welding (GTAW) process for industrial applications is constantly increasing and became an essential tool for better quality and high productivities. Recently, advances in welding technology have focused on improving performance and overcoming the limitation of existing process variants / modalities [1]. In the last decades, technological developments regarding the wire feeding equipment and wire feeding techniques in GTAW process have become the interest of several companies [2], [3], [4], and object of study of research groups [1], [5], [6], [7], [8]

In this context, the dynamic wire feeding stands out. According to Pigozzo and Silva [9], dynamic wire feeding (DWF) is a technique in which the wire feeding speed is not constant and can be oscillated, where the wire moves toward and apart from the molten pool with defined frequency and amplitude; or pulsed, when the wire moves only toward the molten pool with different speeds in distinct periods.

One of the first reports about wire oscillation in GTAW was in 1982 [10], where the dynamic wire feeding was used for repairing procedures of aircraft engine seal teeth. According to the author, the wire dabbing permits that a small amount of material is transferred to the molten pool, since it prevents the premature globing at the wire's tip. Silva et al. [11] affirmed the instant wire feed speed, which is higher for dynamic wire feeding than that in continuous wire feeding, prevents wire pre-heating by the arc, reducing the formation of a droplet at the wire's tip. In experiments carried out with wire oscillation frequency of 2 Hz, Silva et al. [12]showed that the dynamic wire feeding permits a stable metal transfer even in low wire feeding speed, condition which in continuous wire feeding would result in droplet transfers. Moreover, Riffel et al. [13], in orbital welding of AISI304L pipes, state that the wire oscillation enhances the process robustness, especially in overhead position, where constant speed wire feed would tend to result in electrode contamination by large wire droplets formed on the wire's tip.

In wire fed GTAW process, as the wire is not fed coaxially to the arc axis, the insertion position also becomes a welding parameter, hence it should not be set arbitrarily. Geng at al. [14] varied the wire insertion angle and wire distance to the substrate to evaluate "T-type" intersection in GTAW wire arc additive manufacturing. The authors show that both parameters directly affect the weld bead, thus, the intersection geometry, since it changes the start and ending position of the weld bead reinforcement. According to Rodriguez et al. [15] the non-coaxial configuration of wire and arc also leads to instabilities when there are variations in welding direction and arc length. The authors state that greater arc lengths demand higher wire feed speeds to provide continuous bridge transfer due to the longer period that the wire travels through the arc before touching the molten pool. Otherwise, droplet metal transfers would occur. Pigozzo and Silva [16] also observed that minimum variations of 1.5° on the insertion angle could change the continuous bridge transfer mode to intermittent bridge transfer, and a 3° variation could lead to a coarse droplet formation at the wires tip.

Besides positioning, the operational boundaries and conditions for stable metal transfer and sound procedures of wire fed GTAW process also depend on the wire feeding speed. Figueiroa et al. [17], in a study on wire fed GTAW orbital procedures, have raised a ratio between wire feed speed and arc energy, to determine conditions in which the metal transfer would be continuous bridge mode. [18], for the TOPTIG GTAW process variant, classify two metal transfer modes based on wire feeding speed as "continuous liquid flow" and "drop mode". The authors state the drop frequency can be varied by adjusting wire feeding speed, which also have influence over the dropping frequency. Higher wire feed speed led to continuous liquid transfer, until the process starts to be unstable (for very high wire feed speed).

In this context, the control of the wire feeding through the arc and puddle is one of the many challenges of automatizing GTAW process. Furthermore, new wire feeding techniques, such as dynamic wire feeding, makes the process even more complex, demanding a more accurate and extensive monitoring.

The studies approaching wire feeding in GTAW process available in literature are mainly focused on the process influences over the weld beads. The present work aims to characterize the wire feeding technique by means of data acquisition monitoring and high-speed videography. Influences of wire feeding parameters over the weld bed geometry and microstructure will not be evaluated. The understanding of the electrical signals' behavior, associated to the wire feeding monitoring, is crucial for better controlling and automating GTAW process, especially the metal transfer events and process stability.

2. Materials and methods

Single beads of 309LSi stainless steel (AWS ER 309 LSi) wire with 1.0 mm in diameter were laid in ASTM A36 low carbon steel plates with a thickness of 3/8" (9.52 mm). For shielding gas, pure argon (99.99 % level of purity) was used, and the tungsten electrode was an Abicor Binzel E3 (W + 1.5% La_2O_3 + 0.08% ZrO_2 + 0.08% Y_2O) with 3.2 mm in diameter and 40° sharpening angle. In the present work, the wire was inserted in the arc/molten pool through its back region in cold wire configuration. The wire feeding angle was fixed in 20° relative to the electrode axis, parallel to the electrode tip cone surface and the distance electrode-to-wire (D_{EW}) was 1 mm. This configuration promotes the wire feeding through the top regions of the arc closely to the electrodes tip.

The welding procedures were executed in flat position by means of a three axes cartesian system for torch and specimen displacement. In the experiments, the torch was kept stationary, and the substrate plate was displaced through the arc. The power source used was a multi-process IMC Digiplus A7 AC 450. The wire longitudinal oscillation was controlled by the dynamic wire feeding module, developed by Labsolda - Welding and Mechatronics Institute, which allows the wire oscillation with frequencies adjustments up to 20 Hz and amplitudes up to 20 mm. The welding current (I), arc voltage (U_{ARC}), electrode-to-wire voltage (U_{EW}) and wire speed (WS) were acquired by means of a data acquisition system at a sampling rate of 2 kHz. The acquired data was later processed and analyzed in the MATLAB software. Fig 1 shows the experimental set up.

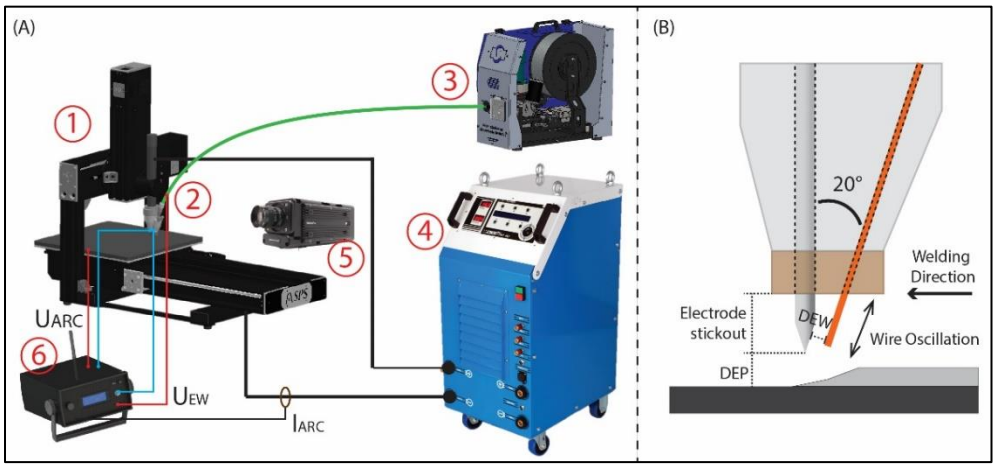

Fig 1 Schematic experimental setup. (A) 1 - Torch displacement systems (SCS); 2 - Low wire insertion angle torch nozzle; 3 - Wire feeder and oscillation unit; 4 - Power source; 5 - High-speed camera; 6 - Data acquisition system. (B) Schematic diagram of wire and electrode position

For high-speed videography an IDT Y4-D2 camera with CAVILUX HF LASER lighting assist was used. The videos were recorded with a resolution of 1024 x 1024 px in a sampling rate of 2000 fps.

3. Results and discussions

1.1. On the process monitoring

Fig 2 shows the characteristic oscillogram of GTAW process with dynamic wire feeding and constant current. In addition to the arc voltage (U_{ARC}) and current (I) signal (usually measured signals), the electrode-to-wire voltage (U_{EW}) acquisition allows to monitor the metal transfer for each cycle of wire oscillation within the process. The high and low levels of U_{EW} represents the metal bridge establishment and detachment respectively. In frame 1, the wire is stationary in its maximum recoil. Frame 2 represents the moment of contact in between the wire and molten pool. In this condition, its electrical potential coincides with the work piece, hence, the electrode-to-wire voltage signal is closer to the arc voltage value which, at the same time, has a small drop because of the arc length reduction due to the arc anchoring on the wire. This behavior was also reported by other authors [11], [16]. When the metal bridge is broken (frame 3) the U_{EW} value drops down and U_{ARC} is increased.

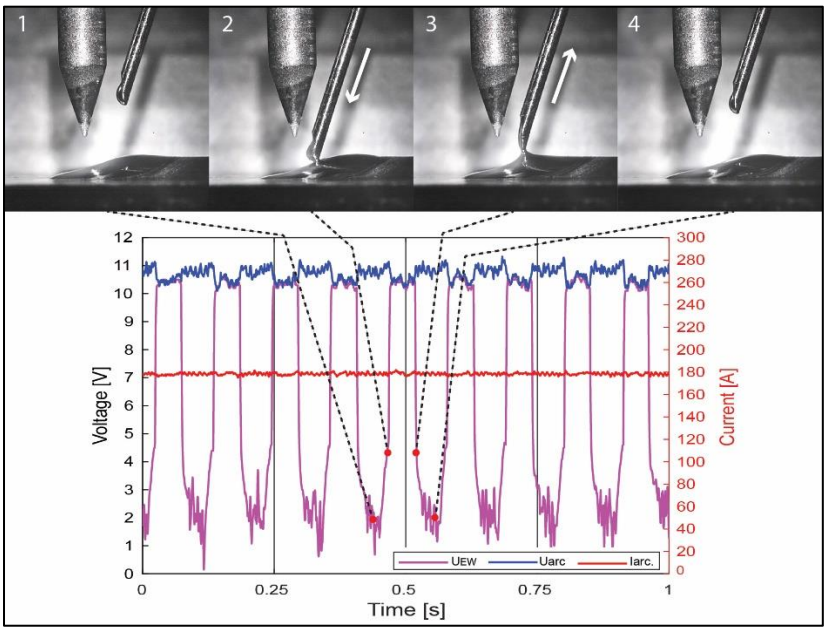

Fig 2 Characteristic oscillogram of GTAW with dynamic wire feeding. Arc voltage (U_{ARC}), Electrode-to-wire voltage (U_{EW}) and Current (I_{ARC})

The abrupt signal variation of the electrode-to-wire voltage permits to accurately identify the instant of the metal bridge establishment and rupture. With data post-processing, many indirect parameters (parameters which are not adjusted) within the dynamic wire feeding technique could be measured. To characterize the GTAW process with dynamic wire feeding, the parameters listed in Table 1 were defined.

Table 1 – GTAW with dynamic wire feeding electrical indirect parameters

Parameter	Description
U_{BDG*} [V]	Average of instant U_{ARC} during metal bridge
U_{DET**} [V]	Average of instant U_{ARC} while metal bridge is detached
U_{W_BDG} [V]	Average of instant U_{EW} during metal bridge
U_{W_DET} [V]	Average of instant U_{EW} while metal bridge is detached
P_{BDG} [W]	Average of instant arc power during metal bridge
P_{DET} [W]	Average of instant arc power while metal bridge is detached

* Bridge; ** Detach

Fig 3 shows the U_{EW} (magenta) superimposed to the wire speed (WS - green) synchronized to the high-speed video frames. By convention, positive velocity represents the forward movement of the wire, then, negative values mean that the wire is being pulled back. In Frame 1, the wire is in its maximum recoil and the speed in zero. As the wire moves forward, it reaches the maximum speed (frame 2) before touching the molten pool. At frame 3, the metal bridge is established during the

deceleration period of the forward movement. In between frames 3 and 4, the wire is still fed into the molten pool and the length of wire inserted toward the molten pool during the metal bridge was defined as “wire’s dip”. At frame 4, although the wire starts the backward movement, the metal bridge is still maintained, and its rupture occurs when the maximum backward speed is reached (frame 5 to 6). The length of wire pulled back still in metal bridge was defined as “bridge recoil”. In adittion, by means of the high-speed videography, the “molten pool elongation” could be evaluated, and it consists on the length of molten metal pulled by the wire by surface tension (highlighted in frame 5). When the wire reaches the maximum recoil, the metal transfer cycle restarts.

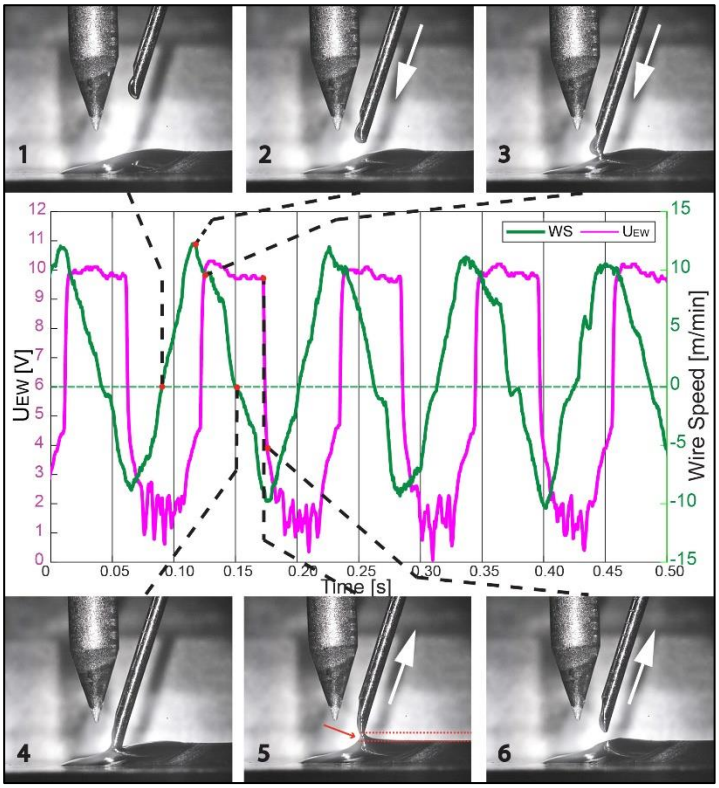

Fig 3 Wire speed (WS – green) and Electrode-to-wire voltage (U_{EW} – magenta) of GTAW with dynamic wire feeding process

Correlating both WS and U_{EW} signals, indirect parameters regarding the metal transfer were defined and are listed in Table 2.

Table 2 - GTAW with dynamic wire feeding metal transfer indirect parameters

Parameter	Description
WFS_{fwd} [m/min]	Average of forward speed
WFS_{m_fwd} [m/min]	Average of maximum forward speed
WFS_{bwd} [m/min]	Average of backward speed
WFS_{m_bwd} [m/min]	Average of maximum backward speed
A_{fwd} [mm]	Average of wire forward amplitude

A_{bwd} [mm]	Average of wire backward amplitude
W_{dip} [mm]	Length of wire fed into the molten pool after metal bridge establishment
Elg [mm]	Length of molten metal pulled by surface tension
B_r	Length of wire pulled back still in metal bridge
MT_{vol} [mm]	Average volume of wire transferred in one metal transfer cycle
T_{bdg} [ms]	Period while the metal bridge occurs
T_{det} [ms]	Period while metal bridge is detached

The electrode-to-wire voltage signal is also useful to monitor the wire insertion position relative to the electrode and to the molten pool. In cases of fixed insertion angle arrangements, as in the present work, the distance from electrode to wire (D_{EW}), pointed out in Fig 1, can be adjusted by varying the electrode stick out from the nozzle, and it determines the wire insertion configuration, considering that the arc length fixed.

Fig 4 shows the $U_{ARC,}$ U_{EW} signals and WS for different conditions of electrode-to-wire distance (1.0, 1.5 and 2.0 mm). As it can be seen both the U_{ARC} and U_{EW} varies with the D_{EW}. The U_{ARC} greater variation is related to the arc anchoring at the wire, as already described. The smaller the D_{EW} is, the greater will be the arc voltage variation, which means that the arc is shorter when the metal bridge occurs.

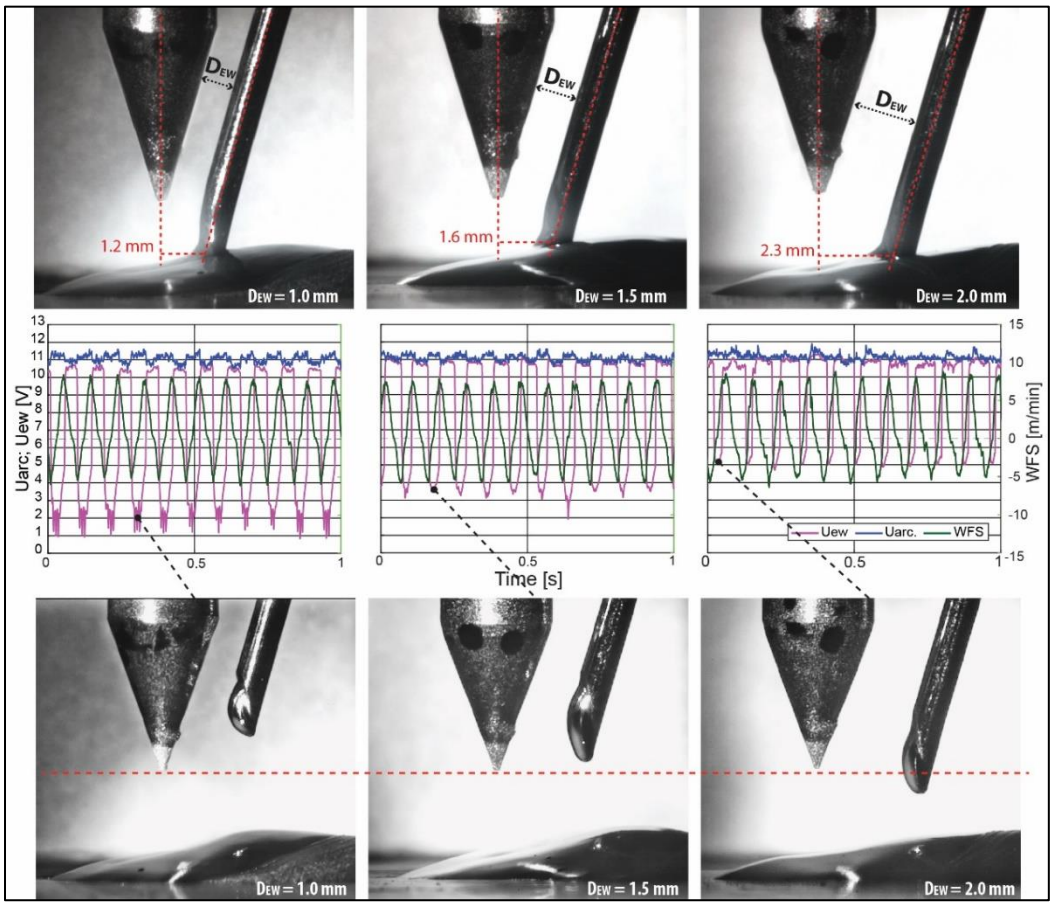

Fig 4 Variation of U_{EW} e U_{ARC} signal with the electrode-to-wire distance. a) D_{EW} = 1.0 mm; b) D_{EW} = 1.5 mm; c) D_{EW} = 2.0 mm

The lower level of the electrode-to-wire voltage signal, even when the metal bridge is detached, is due to the fact that the wire tip remains inside an ionized region, i.e., still inside the arc, in its peripheral region. Fanara and Vilarinho [19] defined the external electrical radio of the arc by using a Langmuir probe in floating condition (not energized). As the probe, or in this case, the wire, enters the current-carrying region of the arc, the voltage signals start to rise, as shown in Fig 5. In frame 1, when the wire is in its maximum recoil (frame 1) the U_{EW} is in its lowest level. As the wire approaches the

arc/molten poll, the U_{EW} arises, and when the metal bridge is stablished (frame 4), the U_{EW} suddenly reaches its peak.

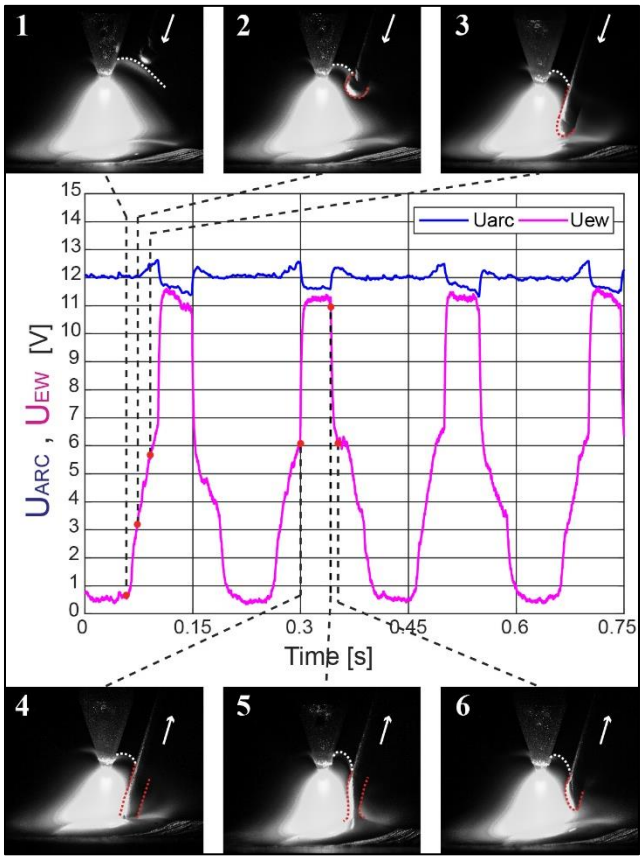

Fig 5 Electrode-to-wire voltage variation with the wire position within the arc

As it can be seen in Fig 4, for the greater D_{EW}, the lowest level of U_{EW} is higher than for the D_{EW} of 1.0 mm. In the frames below the graphs, it is noticeable that the wire, in its maximum recoil position, is closer to the molten pool, and to the arc, for the greater D_{EW}. Although the wire oscillation amplitude was the same for the three cases, for the D_{EW} of 2.0 mm the wire retreated less. This can be explained by the following reason: when the wire is closer to the electrode, in hotter regions of the arc, the melting rate is higher and the wire melts as it dives into the molten pool. In this case, when the backward movements start, the wire tip is next to the molten pool surface. In the third case (DEA 2.0 mm), the melting rate is lower, and the wire dives deep into the molten pool and, in some cases, collides with the solid metal at the bottom (wire stubbing). Moreover, when the backward movements start, the wire tip is located in a lower region inside the molten pool.

Besides the variation of the $D_{EW,}$ the oscillation amplitude also affects the electrode-wire voltage signal. The greater is the pullback amplitude, the lower is the minimum U_{EW} value, because the wire tip reaches more remote regions of the arc, with lower ionization degree. Therefore, to monitor the wire

insertion position, the electrode-to-wire voltage must be analyzed together with the wire feeding parameters raised in Table 2.

1.2. On the wire speed

The dynamic wire feeding is characterized by the arc longitudinal oscillation with defined amplitude and frequency. Is the present work, the resulting wire speed (WS) is and association of the wire's oscillations speed (W_{OS}), promoted by the wire oscillation module, and the wire constant feed speed (W_{CS}) adjusted in the power source, and it can be described by the Equation (1):

$$WS = \mathrm{Wos} + Wcs \qquad (1)$$

The oscillatory wire speed is a sinusoidal function and can be described by:

$$Wos = A\pi f.\cos(2\pi ft) \qquad (2)$$

hence:

$$WS = (A\pi f.\cos(2\pi ft))/(16.67) + Wcs \qquad (3)$$

where *A (mm)* is the oscillation amplitude, *f (Hz)* is the oscillation frequency and *t (s)* is time.

Fig 6 (left) shows separately the two components of the wire speed, and Fig 6 (right), shows the resultant wire speed, as specified by Equation (3). The hypothetical scenario represents a wire oscillation with frequency of 5 Hz, amplitude of 5 mm and wire feeding speed of 1.5 m/min.

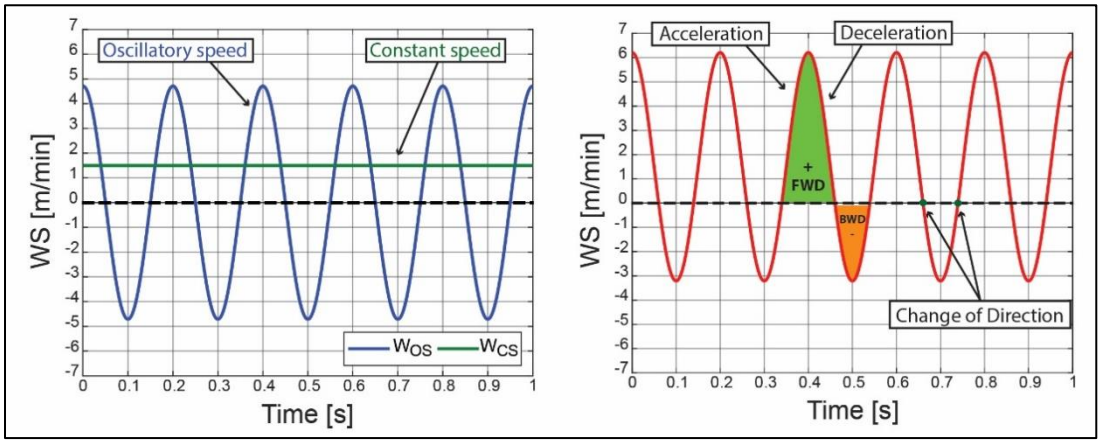

Fig 6 The two components of Wire feed speed. Left) Wire oscillatory speed and wire constant speed; Right) Resulting wire speed.

By convention, positive values of wire speed represent the forward movement of the wire, which means that the wire moves toward the molten pool. Hence, the negatives are related to backward, and the wire moves away from the molten pool. For each direction, the wire movement is characterized by an acceleration period, peak speed, and then, a deceleration period. When the wire reaches speed of 0 m/min (zero), it means the change of the wire movement direction.

Upon individual consideration of the oscillatory component of wire speed, the forward and backward speeds are the same, and its average speed is equal to zero. When the wire constant feeding speed is added, the forward speed is higher than the backward speed, as shown in Fig 6 (right). In this case, the resultant average wire speed is positive and has the same values as the adjusted wire feeding speed in the wire feeder/power source, which means that the wire is being fed to the process.

With the increase of the wire's oscillation frequency and amplitude, although the average speed remains the same, the maximum forward/backward speed, as well the average forward/backward speed, increase. Fig 7 shows the wire's oscillation speed acquired for tests carried out with frequencies of 5.0, 10.0 and 15.0 Hz and 5.0 mm of amplitude, and Fig 8 shows the oscillation speed for amplitudes of 5, 8 and 10 mm and frequency of 10 Hz. The curves represent only oscillatory component of wire's speed.

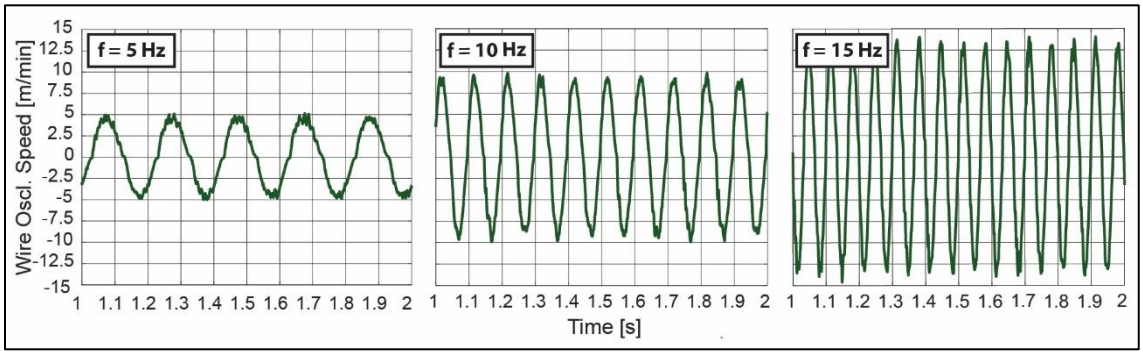

Fig 7 Oscillatory component of wire speed variation with oscillation frequency (Oscillation amplitude set in 5 mm).

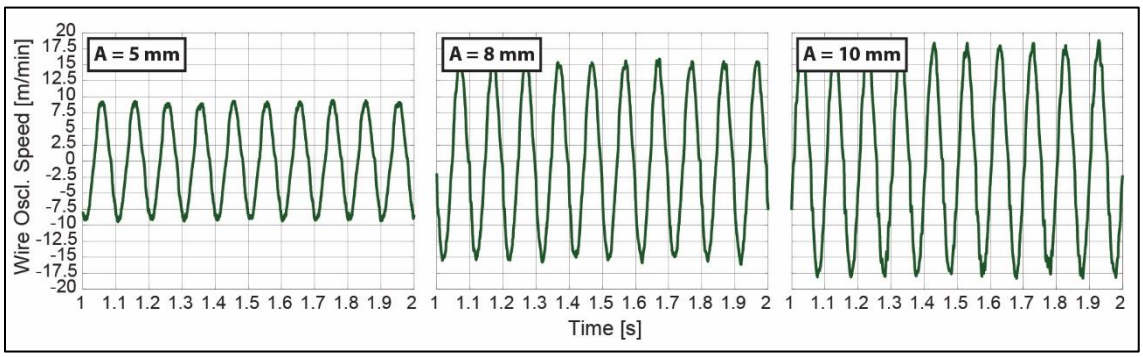

Fig 8 Oscillatory component of wire speed variation with oscillation amplitude (Oscillation frequency set in 10 Hz).

As the average forward and backward speeds varies with the oscillation frequency and amplitude, depending on the frequency, amplitude and wire feeding speed adjusted, there are combinations in which the dynamic wire feeding will not effectively happen, with effective wire delivery to the molten pool. Still considering Equation (3), if the constant component of wire speed is higher than the average backward speed of the oscillatory component, the resultant wire speed is always positive, which means that the pullback movement does not exist. In this way, for each adjusted wire feeding speed, there would be a minimum oscillation frequency, associated to the amplitude, to promote the effective oscillated dynamic wire feeding. In other words, for each combination of frequency and amplitude, there would be a maximum wire feeding speed which would still allow the dynamic wire feeding, as the technique has been described. Fig 9 shows the average backward speed of the oscillation component for different frequencies and amplitudes. The areas bellow the curves represents fields of wire feeding speed settings (as adjusted in the wire feeder) where effective oscillatory dynamic wire feed is provided.

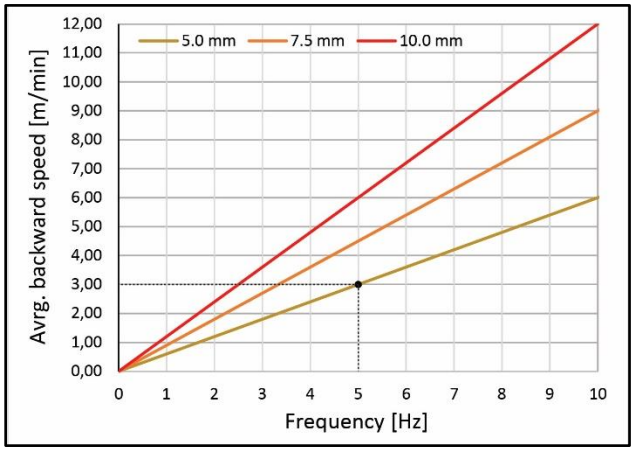

Fig 9 Average backward speed for different oscillation amplitude (5.0, 7.5 and 10.0 mm)

Nevertheless, the adjustment of a wire feed speed below the curves on Fig 9 does not alone guarantee a sound process. In GTAW with dynamic wire feeding there are operational limits regarding the combination of the wire feeding parameters and electrical variables. For a given condition of welding energy, for example, if the wire feed speed adjusted is too low, even though the oscillation state can be indeed achieved, the metal transfer would not occur in every cycle, since the melting rate prevails over the wire feeding rate. Fig 10 shows oscillograms of experiments carried out with 180 A and wire feed speeds of 0.35, 0.45 and 0.65 m/min. The wire oscillation frequency and amplitude were 9.0 Hz and 5.0 mm respectively. As it can be seen, for a very low wire feed speeds, the metal transfer does not occur in every cycle. For 0.35 m/min, it was necessary three cycle to establish the contact in between wire and molten pool. For 0.45 m/min, every two cycles a metal bridge was established, and, for 0.65 m/min, it begun to occur in every cycle.

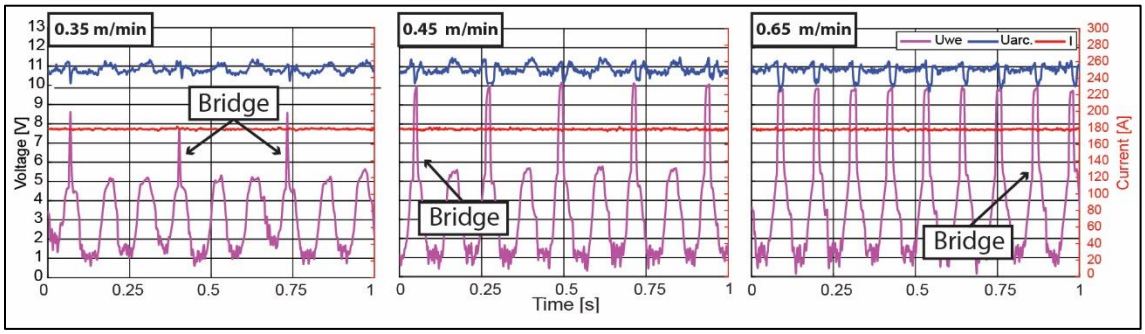

Fig 10 Uarc, Uew and Current oscillograms for different wire feed speed

Although for 0.45 m/min the metal bridge was not established in every cycle, the process was still stable when compared to continuous wire feeding. As it can be seen in Fig 11-right, the continuous wire feeding with low wire feed speed, and constant current tends to create a coarse droplet on the wire's tip due to the low forward speed. In this situation, the wire feeding and melting rate are not in balance. By main influences of electromagnetic forces and plasma flow, the droplet starts a rotational movement, facilitating the electrode contamination. In the dynamic wire feeding Fig 11-left, due to the higher wire speed during the forward and backward movement, the thermal influences of the arc over the wire are reduced and the droplet in the wire's tip is much smaller.

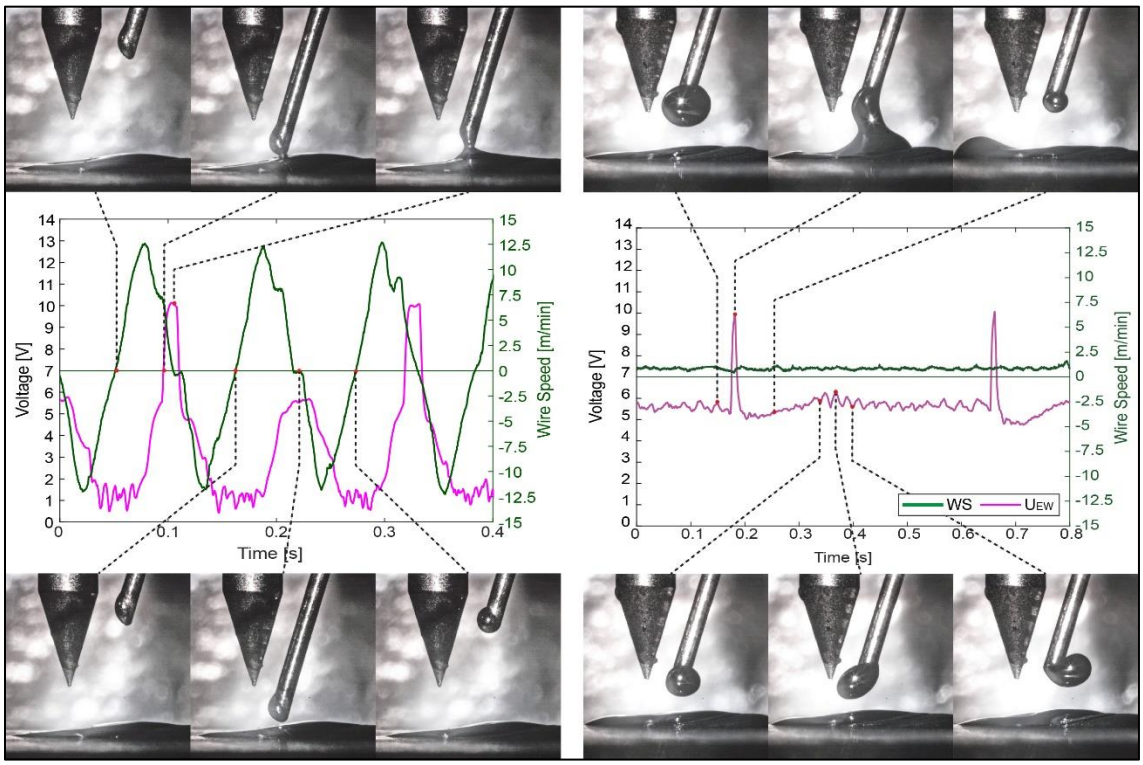

Fig 11 GTAW with low wire feed speed (0.45 m/min) oscillograms and high-speed frames. Left) Dynamic wire feeding; Right) Continuous wire feeding

On the other hand, a high wire feed speed also leads to an instable metal transfer. During the forward movement, the dip of the wire is deeper for higher wire feed speeds, and the wire collides with the solidified metal at the bottom of the molten pool. This phenomenon is also known as stubbing.

Fig 12-left shows the wire stubbing for 1.6 m/min of wire feed speed, 3 Hz and 5 mm of oscillation frequency and amplitude. When the wire reaches the solid metal (frame 3), the wire speed is reduced, and the wire is forced to deviate its trajectory and experiences buckling. In frame 4 it is possible to see that the wire approaches the electrode and the wire feed speed decelerate abruptly. In frame 5, the wire speed shows a sudden peak, and it can be explained by the following reason: as the wire collides with solid metal at the bottom of the molten pool, besides its buckling, an amount of wire was also accumulated inside the wire liner, adding up elastic potential energy. When the wire speed is reduced, its melting rate would prevail over the feeding rate, the once solid stubbing wire melts and loses rigidity and, hence, presents no further resistance to the forward movement of the wire. Then, the wire can be released, giving off the accumulated elastic potential energy, resulting in a sudden speed peak. Each collision can be monitored by the wire speed acquisitions and is represented by and abrupt reduce of wire speed. The U_{EW} signal also shows a small drop when the wire collides and approaches the electrode. In extreme situation the wire could collide the electrode, favoring its contamination.

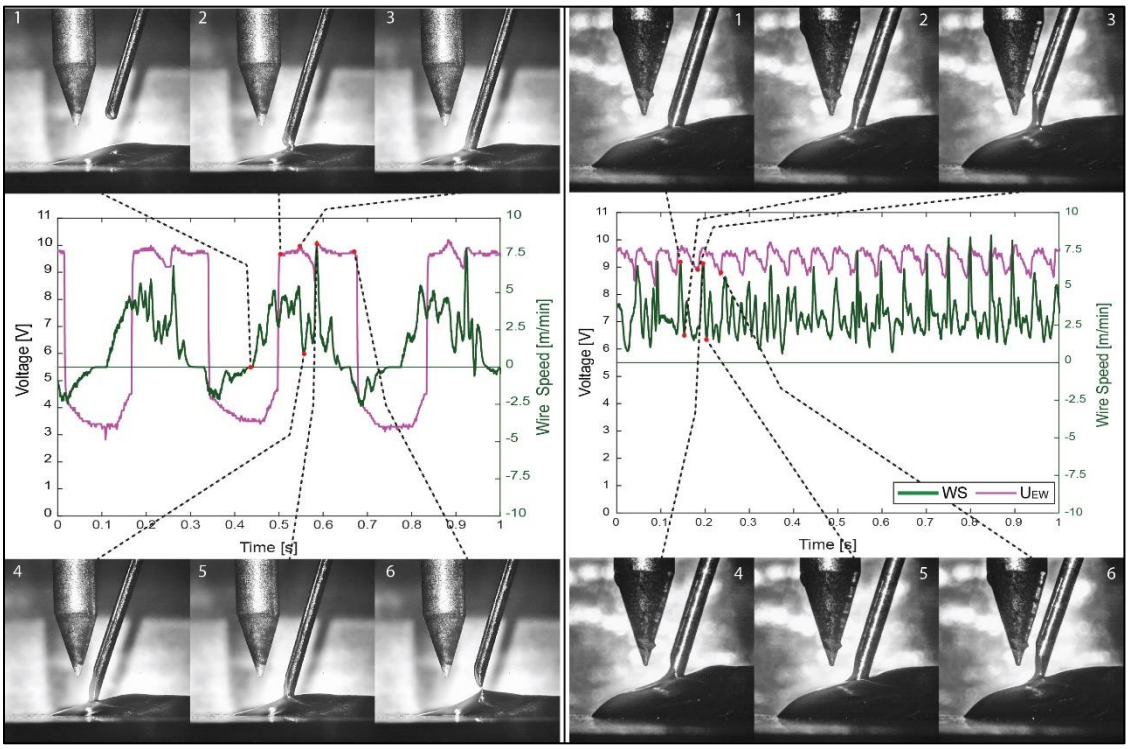

Fig 12 U_{EW} and WS oscillograms for wire stubbing. Left) Dynamic wire feeding; right) continuous wire feeding

Although the wire stubbing leads to instabilities in the metal transfer, up to certain levels it could be tolerable. For conventional wire feeding, the stubbing transfer could be more severe as for process instability, since in dynamic wire feeding the deceleration and inversion of wire direction helps to soften the wire collisions. In Fig 12-right, conventional wire feeding with 2.8 m/min of wire feeding speed was used and, as it can be seen, the wire peaks and valleys are also present, representing the frequent wire collisions and releases in a much higher frequency than for dynamic feeding. The higher number of stubbing events also represents a higher risk of accidental electrode-wire contact for the conventional technique. In both examples, the wire speed peaks reach up to 8 m/min, and it is much higher than the average wire feeding speeds.

Fig 13 shows the spattering promoted by the wire stubbing. Fig 13 A) shows two superimposed frames with a time gap of 0.5 ms, where the wire dislocation is highlighted (1.3 mm). The measured speed of the wire lateral sliding reached, approximately, 156 m/min (2600 mm/s).

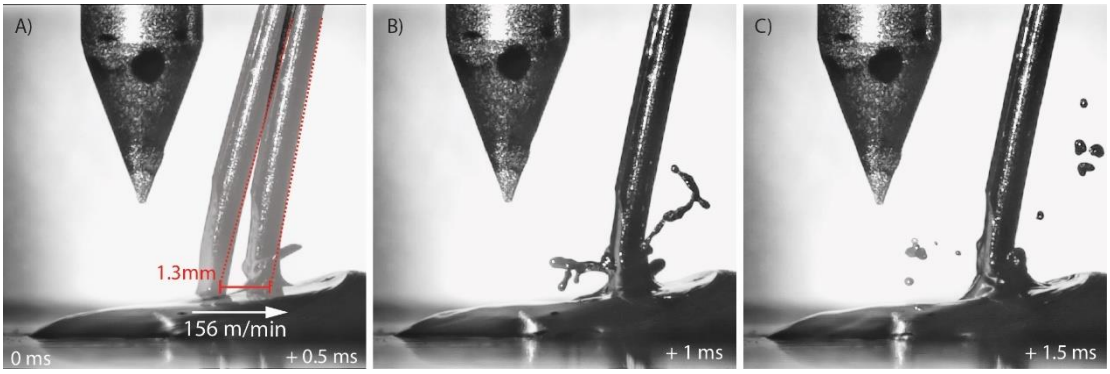

Fig 13 Molten metal spattering caused by wire stubbing

Figure 1 – Molten metal spattering caused by wire stubbing.

For a stable metal transfer and sound weld beads, free of geometrical distortions and spatters, the wire stubbing should be avoided, even though, Zhao et al. [20] for conventional wire feeding in laser cladding application, classified it as “wire stubbing transfer mode”. For dynamic wire feeding with longitudinal wire oscillation, because of the wire’s pullback movement, the metal transfer is always interrupted bridge transfer, as described by Pigozzo et al. [9]. In this case, although wire collision may happen, the metal transfer is still interrupted bridge transfer.

4. Conclusions

The GTAW variants with dynamic wire feeding represent both great potential for exciding in different industrial applications but also higher complexity in the form of extra parameters inherent to the technique. These parameters must be known and registered by researchers and technicians to make them replicable. This work focused on naming and describing each relevant parameter related to dynamic wire feeding in GTAW applications.

The electrode-to-wire voltage conciliated to the wire feed speed signal monitoring, proved to be an effective tool to accurately define and measure the metal transfer cycles and process stability. The sudden variation of the U_{EW} signal accurately detect events within the process and allows the definition of indirect parameters to better characterize the metal transfer. Furthermore, filler wire positioning and metal transfer perturbations can be detected by the electrical signal acquisition and managed to avoid, e.g., electrode contamination or weld bead geometrical distortions. Wire stubbing is properly detected with this technique and can be avoided with fine-tuning of either main wire feeder speed or welding current, increasing robustness, and facilitating process parametrization.

The impact of GTAW-DWF parameters behavior is determinant for process stability and weld result. Although GTAW-DWF techniques have been increasingly offered in the market, knowledge, and tools for GTAW-DWF process characterization were not available. The developed characterization techniques, which extract process features of the GTAW-DWF, may be used not only to support process parameterization for different welding conditions and applications, but also may the base for process online control and weld quality control as well.

5. Acknowledgements

The authors are grateful to PETROBRAS and to the Brazilian government agencies CNPq and CAPES for promoting and founding this work.

6. Conflict of interest statement

There is no actual or potential conflict of interest including any fnancial, personal or other relationships with other people or organizations that could inappropriately infuence, or be perceived to infuence, the present work.

7. References

[1] Da Cunha TV, dos Santos FJ, Voigt AL (2022) Study on the influence of operational conditions on weld bead morphology produced through TIG process with longitudinal wire oscillation. Journal of the Brazilian Society of Mechanical Sciences and Engineering 44:292. https://doi.org/10.1007/s40430-022-03582-z

[2] Fronius (2022) Dynamic wire - TIG cold wire welding [Brochure]. Available in: https://www.fronius.com

[3] EWM (2018) TigSpeed TIG cold/hot wire welding [Brochure]. Available in: https://www.ewm-group.comendownloads.html

[4] TipTIG TipTIG - The evolution of TIG welding [Brochure]. Available in: https://www.tiptig-europe.eu/en/tiptig-technologie.html

[5] Jorge VL, Santos CHA, Scotti FM, Larquer TR, Mota CP, Reis RP, Scotti A (2018) Development and evaluation of wire feeding pulsing techniques for arc welding. Soldagem e Inspecao 23:326–339. https://doi.org/10.1590/0104-9224/SI2303.03

[6] das Neves N, Fernandes MF, Von Dollinger CF de A, Assis JMK, Voorwald HJC (2022) Effects of GTAW Dynamic Wire Feeding Frequencies on Fatigue Strength of ASTM A516-70 Steel Welded Joints. J Mater Eng Perform 31:6435–6450. https://doi.org/10.1007/s11665-022-06868-4

[7] Riffel KC, e Silva RHG, Haupt W, da Silva LE, Dalpiaz G (2020) Effect of dynamic wire in the GTAW process: Microstructure and corrosion resistance. J Mater Process Technol 285:116758. https://doi.org/10.1016/j.jmatprotec.2020.116758

[8] Henrique Gonçalves Silva R, Correa Riffel K, Pompermaier Okuyama M, Dalpiaz G (2019) Effect of dynamic wire in the GTAW process. J Mater Process Technol 269:91–101. https://doi.org/10.1016/j.jmatprotec.2019.01.033

[9] Pigozzo IO, e Silva RHG, Galeazzi D, Pereira AS (2022) Pulsed dynamic wire feeding with low insertion angle in GTAW process: a metal transfer characterization. Welding in the World 66:2107–2118. https://doi.org/10.1007/s40194-022-01352-y

[10] Rudy JF (1982) Development and Application of Dabber Gas Tungsten Arc Welding for Repair of Aircraft Engine, Seal Teeth

[11] Silva RHG e, Silva RGN, Schwedersky MB, Dalpiaz G, Dutra JC (2019) Contributions of the High Frequency Dynamic Wire Feeding in the GTAW Process for Increased Robustness. Soldagem & Inspeção 24:. https://doi.org/10.1590/0104-9224/si24.30

[12] Silva RHG, dos Santos Paes LE, Okuyama MP, de Sousa GL, Viviani AB, Cirino LM, Schwedersky MB (2018) TIG welding process with dynamic feeding: a characterization approach. The International Journal of Advanced Manufacturing Technology 96:4467–4475. https://doi.org/10.1007/s00170-018-1929-6

[13] Riffel KC, Silva RHG e, Dalpiaz G, Marques C, Schwedersky MB (2019) Keyhole GTAW with Dynamic Wire Feeding Applied to Orbital Welding of 304L SS Pipes. Soldagem & Inspeção 24:. https://doi.org/10.1590/0104-9224/si24.18

[14] Geng H, Li J, Xiong J, Lin X, Zhang F (2017) Optimization of wire feed for GTAW based additive manufacturing. J Mater Process Technol 243:40–47. https://doi.org/10.1016/j.jmatprotec.2016.11.027

[15] Rodriguez N, Vázquez L, Huarte I, Arruti E, Tabernero I, Alvarez P (2018) Wire and arc additive manufacturing: a comparison between CMT and TopTIG processes applied to stainless steel. Welding in the World 62:1083–1096. https://doi.org/10.1007/s40194-018-0606-6

[16] Pigozzo IO, Gonçalves e Silva RH, Wallerstein D (2022) On Orbital GTA Root-Pass Welding: Evaluation of AVC Performance, Bevel Geometry Influence and Wire Feed Technique. Soldagem & Inspeção 27:. https://doi.org/10.1590/0104-9224/si27.12

[17] Figueirôa DW, Pigozzo IO, Silva RHG e, Santos TF de A, Urtiga Filho SL (2017) Influence of welding position and parameters in orbital tig welding applied to low-carbon steel pipes. Welding International 31:583–590. https://doi.org/10.1080/09507116.2016.1218615

[18] Opderbecke T, Guiheux S (2009) TOPTIG: robotic TIG welding with integrated wire feeder. Welding International 23:523–529. https://doi.org/10.1080/09507110802543146

[19] Fanara C, Vilarinho L (2004) Electrical characterization of atmospheric pressure arc plasmas. Eur Phys J D At Mol Opt Phys 28:241–251. https://doi.org/10.1140/epjd/e2003-00301-8

[20] Zhao S, Xu S, Yang L, Huang Y (2022) WC-Fe metal-matrix composite coatings fabricated by laser wire cladding. J Mater Process Technol 301:117438. https://doi.org/10.1016/j.jmatprotec.2021.117438